



Diffuse Hydrothermal Venting: A Hidden Source of Iron to the Oceans

Alastair J. M. Lough^{1,2*}, Douglas P. Connelly², William B. Homoky³, Jeffrey A. Hawkes^{1†}, Valerie Chavagnac⁴, Alain Castillo⁴, Majid Kazemian⁵, Ko-ichi Nakamura⁶, Tohru Araki⁵, Burkhard Kaulich⁵ and Rachel A. Mills¹

¹ Ocean and Earth Science, National Oceanography Centre Southampton, University of Southampton, Southampton, United Kingdom, ² National Oceanography Centre, European Way, Southampton, United Kingdom, ³ Department of Earth Sciences, University of Oxford, Oxford, United Kingdom, ⁴ GET CNRS UMR5563, Geosciences Environnement Toulouse, University of Toulouse, Toulouse, France, ⁵ Diamond Light Source Ltd., Didcot, United Kingdom, ⁶ National Institute of Advanced Industrial Science and Technology, Tsukuba, Japan

OPEN ACCESS

Edited by:

Antonio Tovar-Sanchez,
Spanish National Research Council
(CSIC), Spain

Reviewed by:

Aridane G. Gonzalez,
Instituto de Oceanografía y Cambio
Global (IOGAG), Spain
Juan Santos Echeandia,
Instituto Español de Oceanografía
(IEO), Spain

*Correspondence:

Alastair J. M. Lough
A.J.M.Lough@soton.ac.uk

†Present address:

Jeffrey Alistair Hawkes,
Analytical Chemistry, Department
of Chemistry, BMC, Uppsala
University, Uppsala, Sweden

Specialty section:

This article was submitted to
Marine Biogeochemistry,
a section of the journal
Frontiers in Marine Science

Received: 21 February 2019

Accepted: 28 May 2019

Published: 12 July 2019

Citation:

Lough AJM, Connelly DP,
Homoky WB, Hawkes JA,
Chavagnac V, Castillo A, Kazemian M,
Nakamura K-i, Araki T, Kaulich B and
Mills RA (2019) Diffuse Hydrothermal
Venting: A Hidden Source of Iron to
the Oceans. *Front. Mar. Sci.* 6:329.
doi: 10.3389/fmars.2019.00329

Iron (Fe) limits primary productivity and nitrogen fixation in large regions of the world's oceans. Hydrothermal supply of Fe to the global deep ocean is extensive; however, most of the previous work has focused on examining high temperature, acidic, focused flow on ridge axes that create "black smoker" plumes. The contribution of other types of venting to the global ocean Fe cycle has received little attention. To thoroughly understand hydrothermal Fe sources to the ocean, different types of vent site must be compared. To examine the role of more diffuse, higher pH sources of venting, a hydrothermal plume above the Von Damm vent field (VDVF) was sampled for Total dissolvable Fe (unfiltered, TDFe), dissolved Fe (<0.2 μm , dFe) and soluble Fe (<0.02 μm , sFe). Plume particles sampled *in situ* were characterized using scanning electron microscopy and soft X-ray spectromicroscopy. The VDVF vents emit visibly clear fluids with particulate Fe (TDFe-dFe, >0.2 μm) concentrations up to 196 nmol kg^{-1} comparable to concentrations measured in black smoker plumes on the Mid-Atlantic Ridge. Colloidal Fe (cFe) and sFe increased as a fraction of TDFe with decreasing TDFe concentration. This increase in the percentage of sFe and cFe within the plume cannot be explained by settling of particulates or mixing with background seawater. The creation of new cFe and sFe within the plume from the breakdown of pFe is required to close the Fe budget. We suggest that the proportional increase in cFe and sFe reflects the entrainment, breakdown and recycling of Fe bearing organic particulates near the vents. Fe plume profiles from the VDVF differ significantly from previous studies of "black smoker" vents where formation of new pFe in the plume decreases the amount of cFe. Formation and removal of Fe-rich colloids and particles will control the amount and physico-chemical composition of dFe supplied to the deep ocean from hydrothermal systems. This study highlights the differences in the stabilization of hydrothermal Fe from an off-axis diffuse source compared to black smokers. Off-axis diffuse venting represent a potentially significant and previously overlooked Fe source to the ocean due to the difficulties in detecting and locating such sites.

Keywords: iron, colloid, nanoparticle, hydrothermal, Von Damm, GEOTRACES

INTRODUCTION

At present there are several known types of hydrothermal system. The most widely discovered type are black smokers that are located at ridge axes and emit acidic pH (2–5), high temperature (up to 400°C) metal rich fluids. The extent of metal enrichment in these vents varies depending on the host rock through which seawater transformed into hydrothermal fluid circulate. Ultramafic hosted vent sites such as Rainbow on the Mid-Atlantic Ridge (MAR) have higher Fe concentrations relative to sulfide, while basalt hosted systems tend to have low Fe:H₂S ratios (Severmann et al., 2004). Other less frequently observed venting at/near ridge axes include white smokers that emit lower temperature (up to 300°C), acidic Zn rich fluids (Tivey et al., 1995) and low temperature (<40 to 90°C) high pH (9–11) alkaline vents that emit hydrogen and methane rich fluids from calcium carbonate chimneys (Kelley et al., 2005). Seafloor venting also occurs further away from ridge axes on seamounts and in calderas associated with island arcs (Butterfield et al., 2011; Hawkes et al., 2014) and other submarine volcanic edifices (McCarthy et al., 2005; Aquilina et al., 2014; Lemaitre et al., 2014; Rizzo et al., 2016; Santana-González et al., 2017; Guieu et al., 2018). The Von Damm vent field (VDVF) is a new type of hydrothermal system located away from the ridge axis emitting clear, moderately low pH (6–7) fluids with temperatures up to 215°C (Hodgkinson et al., 2015). This style of venting is chemically similar to diffuse venting that seeps from the seafloor in areas where there is hydrothermal activity. Seawater percolates through fissures in the seafloor mixing with hydrothermal fluids in the sub-surface resulting in lower temperature, lower metal content, less acidic pH fluids compared to the focused flow from chimneys. These lower temperature fluids account for 50 to 90% of the hydrothermal volume flux (German, 2016) and ~70% of the hydrothermal heat flux (Elderfield and Schultz, 1996; German et al., 2015) and both of these fluxes remain poorly quantified. Therefore, the flux of trace metals from these systems is also poorly constrained as a result of uncertainties in the volume flux and no previous investigations into the behavior of metals as diffuse fluids mix with seawater (Tagliabue and Resing, 2016).

Focused hydrothermal venting emits acidic, high temperature fluids from chimneys located along ridge axes (Von Damm et al., 1985; Vondamm and Bischoff, 1987; Von Damm, 1990, 1995). These fluids have high Fe and Mn concentrations (up to 25000 μM Fe and up to 4480 μM Mn) that mix with the surrounding seawater to create particle rich plumes with Fe and Mn concentrations elevated in comparison to the open ocean (>1 nmol kg⁻¹ Fe and >0.1 nmol kg⁻¹ Mn) (Mottl and McConachy, 1990; James and Elderfield, 1996; Field and Sherrell, 2000; Statham et al., 2005; Bennett et al., 2008; Hawkes et al., 2013; Fitzsimmons et al., 2014; Gartman et al., 2014; Lough et al., 2017; Waeles et al., 2017). Following Fe and Mn oxidation kinetics the dissolved Fe (dFe) and Mn (dMn) (<0.45 or 0.2 μM depending on filters used) in these plumes should precipitate as particulates that eventually settle to the seafloor (Millero et al., 1987; Santana-Casiano et al., 2005). Many studies have now shown that plume Fe chemistry cannot be explained by oxidation kinetics alone and a fraction of chemically stabilized Fe will persist in the water

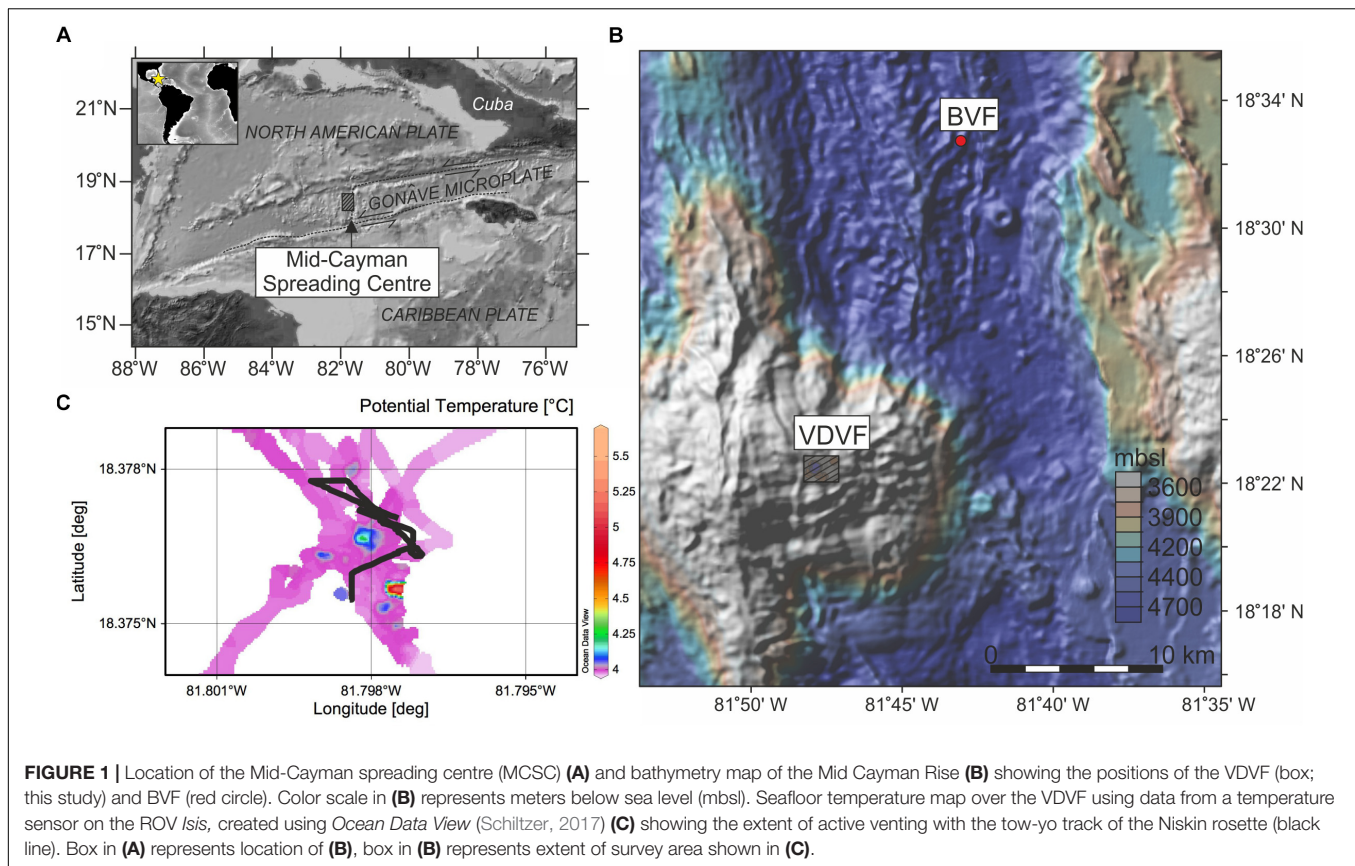
column (Statham et al., 2005; Bennett et al., 2008; Wang et al., 2012; Hawkes et al., 2013; Kleint et al., 2016; Waeles et al., 2017). Hydrothermal plumes therefore have the potential to add dFe to the open ocean if the stabilized dFe can be ventilated into the deep ocean (Tagliabue et al., 2010; Wu et al., 2011; Resing et al., 2015; Fitzsimmons et al., 2017).

Venting plumes that rise above ridge topography are exposed to large scale open ocean water mass movements and can be detected >1000 km (Wu et al., 2011; Fitzsimmons et al., 2014; Resing et al., 2015) away from the ridge axis. This scale of transport is less likely for plumes originating from focused venting along the axial valley of slow spreading ridges. Plumes within axial valleys [or situated at the base of any seafloor depression, i.e., a caldera (Hawkes et al., 2014)] are restricted by the valley walls and these Fe rich waters are therefore sheltered from dispersion by macro scale ocean currents. The only way these Fe rich waters can be transported into the deep ocean is if the plume rises high enough to breach the walls of the valley or by diapycnal mixing over the ridge (Conway and John, 2014; Vic et al., 2018).

Types of diffuse venting that are located away from the ridge axis are considered to be of less importance to global hydrothermal Fe emissions due to the lower Fe and Mn concentrations of fluids emanating from the seafloor. What is frequently overlooked is that despite the lower dFe and dMn concentrations, venting that occurs at shallower depths at the edge or outside of the ridge valley, allows plume waters to be exposed to larger scale water mass movements and areas of enhanced mixing due to tides and turbulence caused by ridge bathymetry which will facilitate export into the deep ocean (Vic et al., 2018). Moreover, even though the initial concentrations of Fe discharged from diffuse venting is lower than that of focused ones, it is possible that these vents could make a globally significant contribution to the hydrothermal Fe flux to the ocean if a larger proportion of the hydrothermal Fe is stabilized. This has been suggested in attempts to model the hydrothermal Fe flux (German et al., 2015).

The true extent of diffuse off-axis venting is largely unknown as most oceanographic surveys searching for new vent sites follow ridge axes using sensors to detect for plume signals. Given that off-axis diffuse sites are likely to be lower in temperature and particle anomalies they are unlikely to be observed using traditional CTD packages and bespoke sensors are required to detect reduced species in the water column (German et al., 2010; Connelly et al., 2012; Baker et al., 2016).

Diffuse fluids emanating from hydrothermal systems represent a potentially important and overlooked source of Fe and Mn to the ocean. The mechanisms of dissolved Fe stabilization and particle formation over these sites are under-investigated in comparison to black smoker type plumes. In this study we investigate the size fractionation and speciation of Fe and Mn in waters over the crest of a slow spreading ridge 13 km west of the ridge axis, where hydrothermal venting has been observed previously (German et al., 2010; Connelly et al., 2012). Specifically, we address the question of how important other styles of venting are as a source of Fe and Mn to the ocean compared to focused flow from black smokers.



MATERIALS AND METHODS

Study Area

Samples were collected aboard the RSS *James Cook* (voyage JC82) from over the Cayman Trough during February 2013. The Cayman Trough is located in the Caribbean Sea south of the Cayman Islands (Figure 1A). The Mid Cayman Spreading Centre (MCSC) is a 110 km long ultraslow spreading ridge (<20 mm year⁻¹) bisecting the Cayman Trough. Spreading was initiated 49 Ma and is continuing at a full spreading rate of 15 mm year⁻¹ (Leroy et al., 2000).

The VDFV is located at 18°22.605'N 81°47.875'W, 13 km west of the MCSC spreading axis and sits atop the Mount Dent, Oceanic Core Complex (OCC) at a depth of 2300 mbsl (Figure 1B). An OCC is a common feature of slow and ultra-slow spreading ridges formed by detachment faulting to accommodate spreading accretion where magmatic supply is insufficient. During the faulting and spreading process crustal (gabbroic) rocks from depth are uplifted exposing mantle rocks (peridotite) (Smith et al., 2006; Escartín et al., 2008, 2017). Due to this uplift the VDFV lies 2700 m above the MCSC axis (Figure 1B).

It has been suggested that the heat required for hydrothermal venting at the VDFV is provided by cooling of the exhumed lower crust at the foot wall of the OCC (Hodgkinson et al., 2015). This makes it different in comparison to more typical hydrothermal systems where the heat source driving circulation is magmatic

(German et al., 2016). The heat source driving hydrothermal venting is therefore an indirect result of magmatism rather than a direct one.

The VDFV consists of four overlapping cones of talc [Mg₃Si₄O₁₀(OH)₂] breccia 20 to 75 m high and 75 to 150 m wide (Copley and Talling, 2013). Hydrothermal fluids vent from a series of talc chimneys and vent fluid data from this expedition has been published previously (Hodgkinson et al., 2015) which we will summarize here (Table 1). The “Spire” is a 3 m tall chimney, which vents clear fluids with a *in situ* temperature of 215°C and pH of 6.1 (measured on board at 25°C). At the base of the spire to the west a 1 m diameter hole (“hotter than hole”) vents 138°C clear fluids with a pH of 6.1. On the southern margin of the largest cone a smaller site of venting named “chimlets” has vent fluids with a temperature of 108°C and a pH of 6.9. On the smallest and southernmost cone, a site named X15 has vent fluids with a temperature of 110°C and a pH of 6.7. There are two other observed sites with venting >43°C along with many areas of lower temperature diffuse venting (Figure 1C). Pock marked regions of sediment which may indicate ongoing and/or historic fluid flow underlying sediments were also observed at the southern and western base of Mount Dent (Hodgkinson et al., 2015).

The vent fluids collected from the VDFV have Cl concentrations (574–643 mmol kg⁻¹) greater than seawater (~546 mmol kg⁻¹) (Table 1) this indicates that the overlying plume has a salinity greater or identical to the background

TABLE 1 | Hydrothermal vent fluid composition at the Von Damm vent field.

Chimney	Temp. (°C)	pH	Cl (mmol kg ⁻¹)	Mg (mmol kg ⁻¹)	Mn (μmol kg ⁻¹)	Fe (μmol kg ⁻¹)	Cu (μmol kg ⁻¹)	H ₂ S (mmol kg ⁻¹)	Flow rate (m ³ s ⁻¹)
Main spire	215	6.0	643	15	8.01	18.9	1.11	0.93	0.05
		6.2	592	32	4.62	6.58	0.46	0.92	
Hotter than Hole	138	6.1	610	27	10.1	138	94.5	0.33	1.18
		6.1	599	26	12.4	604	460	0.44	
		6.2	603	30	14.2	392	289	0.97	
Chimlet 2	108	6.2	601	23	11.2	144	4.56	0.64	0.01
		7.0	574	41	9.6	160	1.39	NA	

NA, not analyzed, Temperature is the maximum temperature recorded from a temperature probe. All data from Hodgkinson et al. (2015). Flow rate is calculated from the vent orifice radius and flow rate presented in Table 4 of Hodgkinson et al. (2015) assuming the vent orifice is circular.

seawater. The vent fluids also show a wide range of trace metal concentrations, which is most likely a result of the variability in seawater-vent fluid mixing in the subsurface prior to venting. Trace metal concentrations do not show a linear relationship with Mg so end-member vent fluid concentrations cannot be calculated by linear regression as is usually done for vents with focused flow (Von Damm et al., 1985; Hodgkinson et al., 2015). The vents on the VDVF have dissolved organic carbon (DOC) concentrations in the range of 134 to 762 μM which is at the higher end of the global range for other vents of 15 to 539 μM, compared to background seawater values of 35 to 48 μM (Hawkes et al., 2015). Based on water volume flow rates (Table 1) the vast majority of plume waters will be derived from the hotter than hole vent. This is mainly a result of the area of the vent orifice which is 0.79 m² and may represent the early genesis of the more typical chimney structure of the Main Spire (area = 0.03 m²).

Hydrographically, the deep water in the Cayman Trench has temperature, salinity and an O₂ concentration similar to North Atlantic Deepwater (NADW) (Connelly et al., 2012; Supplementary Table S1). It is likely that this water enters the Cayman basin via the Oriente Fracture Zone from the Windward Passage (Johns et al., 2002). Due to a lack of oceanographic research in the Caribbean Sea there is little data on the chemistry and movement of deep water masses in the Cayman Trough.

Detecting and Sampling the Hydrothermal Plume

The dispersion of hydrothermal plumes that are not confined to a ridge valley are complicated by tidal movements and open ocean currents. To effectively sample and characterize the dynamic plume over the VDVF, a titanium Niskin rosette with 10 L bottles (*Ocean test equipment*) and an attached sensor package were deployed using a tow-yo strategy. This involves slowly moving the ship over the vent site with the rosette in the water and moving the rosette up and down. The sensor package is then used to differentiate the plume from background seawater based on *in situ* measurement of temperature, Eh [the measure of voltage of an inert (Pt) electrode against reference Ag-AgCl electrode in saturated KCl solution] and light scattering sensors (LSS). Relative to background seawater buoyant rising plume waters will be warmer, have higher concentrations of reducing species (Fe²⁺, Mn²⁺, and H₂S) and a higher concentration

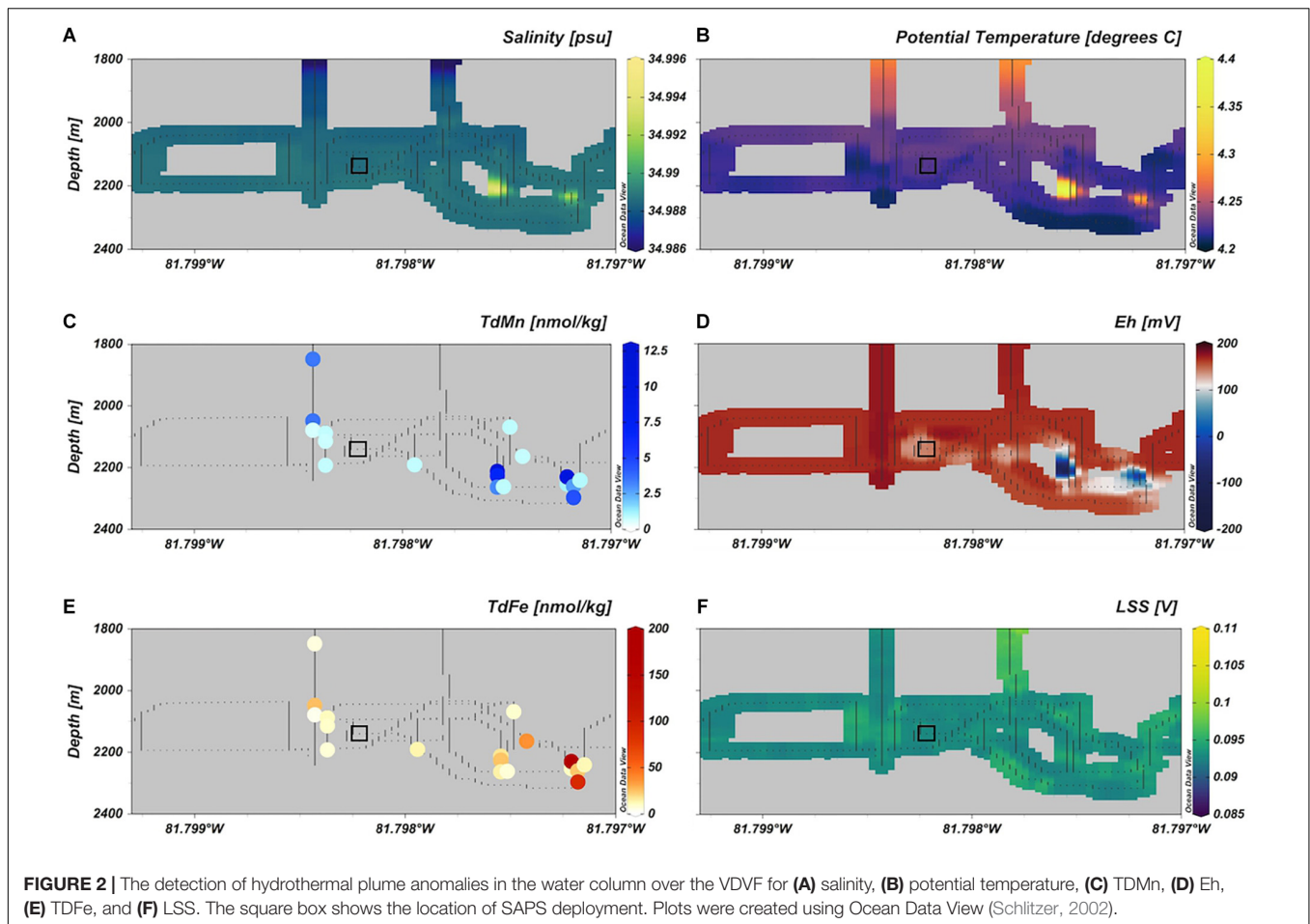
of particulates. The buoyant plume drags up colder bottom waters from beneath during plume rise so typically the non-buoyant plume has a temperature cooler than background seawater along with less pronounced Eh and particle anomalies (Speer and Rona, 1989). This is provided that there is a detectable temperature gradient between entrained deep waters and background seawater at the depth of neutral buoyancy. Sampling depths ranged from 1867 to 2289 mbsl over the VDVF and the tow-yo covered a distance of ~0.5 km and up to ~450 masf (Figure 1C).

Once Niskin bottles were recovered on deck, plume waters were filtered as soon as possible in a clean lab through 0.2 μm polycarbonate filters (Whatman) for the dissolved fraction and 0.02 μm alumina syringe filters (Whatman) for the soluble fraction. An unfiltered aliquot was also taken for the total dissolvable fraction [TD = particles that will dissolve at pH 1.7–1.8 over a period >1 year plus dissolved species (Lough et al., 2017, 2019)]. All samples were stored in acid cleaned low density polyethylene bottles (LDPE) with pH adjusted to 1.7–1.8 using ultra purity HNO₃ (Romil). Mean Fe concentration of background station samples (3494 to 4495 mbsl, ~25 km NE within the Cayman trench) analyzed by flow injection chemiluminescence (Obata et al., 1993) is 1.1 ± 0.2 nmol kg⁻¹ similar to deep ocean Fe concentrations of the North Atlantic deep water (NADW) 0.75 nmol kg⁻¹ (Rijkenberg et al., 2014). This indicates that background waters at this site are likely derived from NADW as expected with additional Fe derived from the Caribbean basin. These background measurements also verify our clean sample handling techniques.

Particles were sampled *in situ* using a stand-alone pumping system (SAPS) attached to the titanium rosette frame, which pumped 945 L of seawater through a polycarbonate filter (1 μm pore size, Whatman, 293 mm) from a low Eh non-buoyant plume at 2140 mbsl (Figure 2). Filters were rinsed on board with de-ionized water (18.2 ΩM, Milli-pore) to remove salts and stored at -20°C.

Determination of Trace Metal Concentrations in Plume Samples

The concentration of Fe and Mn in Total dissolvable, dissolved and soluble plume samples was determined using a standard addition method with semi-automated pre-concentration that has been used previously for seawater samples (Milne et al., 2010;



Billier and Bruland, 2012). The Fe and Mn in samples was extracted by loading 15 ml onto a WAKO chelate resin column (Wako Pure Chemical Industries, Japan), rinsing with 0.05 M Ammonium Acetate (Optima grade, Romil) to remove major ions and eluted by passing 1.5 ml 1 M HNO₃ over the column. This increased the concentration of the analytes by a factor of 10 for HR-ICP-MS analysis to ensure sample signals sufficiently greater than the instrument Limit of detection (l.o.d).

The l.o.d values for Fe and Mn was 0.09 and 0.003 nmol kg⁻¹ (3σ of blank $n = 12$), respectively. To test the method accuracy and precision the NASS-6 seawater reference material (National Research Council Canada) was analyzed for Fe and Mn. Measured values of 9.1 ± 0.7 nmol kg⁻¹ Fe and 8.7 ± 0.6 nmol kg⁻¹ Mn ($n = 6$) compared well to certified values of 8.65 ± 0.81 and 9.39 ± 0.86 nmol kg⁻¹, respectively.

Mineralogy and Oxidation State of Plume Particles by Scanning Electron Microscopy and Soft X-Ray Spectromicroscopy Techniques

The morphology and chemical composition of particles was examined using the backscatter detector on a scanning electron microscope (SEM) (Carl Zeiss LEO 1450VP) and element

composition of particles was determined using an energy dispersive X-ray (EDX) detector (Princeton Gamma Technology Light Element Detector) built-in to the SEM.

Fe bearing particles that did not contain sulfur but showed peaks for oxygen were assumed to be Fe oxyhydroxides. However, the exact mineralogy of these particles cannot be determined due to the uncertainty of EDX analysis for elements as light as oxygen (Goldstein et al., 2003). Due to the time-scales over which plume dilution occurs it is unlikely that more structured Fe oxides such as hematite or goethite will form and Fe oxyhydroxides have been shown to be the most prevailing Fe oxide phase in hydrothermal plumes (Feely et al., 1994; Fitzsimmons et al., 2017; Lough et al., 2017; Hoffman et al., 2018).

The scanning transmission X-ray microscope (SXM) at beamline I08 of the Diamond Light Source synchrotron (United Kingdom) was used to assess the oxidation state of iron in particles by examining the X-ray absorption near-edge structure (XANES). Prior to spectromicroscopy analysis samples were prepared in a glove box flushed with N₂ gas to prevent oxidation of Fe from ambient atmosphere. In the glove box SAPS filter segments were defrosted and placed in de-ionized water to create a suspension of particles. Droplets of this suspension were mounted onto standard (3 mm) mesh grids or silicon nitride membranes. Image stacks of particles were collected at energies

of 700 to 717 eV across the Fe L_3 absorption edge to determine chemical oxidation state of Fe. The near edge peak splitting of XANES spectra indicates the oxidation state of Fe in the sample with the initial peak intensity indicative of Fe(II) content and the preceding peak intensity indicative of Fe(III) content (de Groot, 2009). Based on the difference in the height of these two peaks, regions of particles are separated into four categories: pure Fe(II), Fe(II) rich mixed valence, Fe(III) rich mixed valence, and Fe(III) pure (von der Heyden et al., 2012; Hawkings et al., 2018). Data was processed using the MANTiS (Lerotic et al., 2014) software for background subtraction, image normalization, image alignment and X-ray peak fitting. Results are compared to previously published spectra of Fe minerals (Toner et al., 2009, 2014, 2016; von der Heyden et al., 2012).

Synchrotron X-ray micro-fluorescence (μ XRF) was used to assess the distribution of Fe, C, and O in samples with PyMCA software used to create element maps (Solé et al., 2007). Given that hydrothermal plumes typically have a deficit of particulate inorganic carbon (PIC) and elevated concentrations of particulate organic carbon (POC) compared to seawater (Hoffman et al., 2018) we assume that the majority of carbon in our samples detected by μ XRF is most likely to be organic in nature and not carbonate minerals unless the carbon map appears to be the same as the oxygen map.

RESULTS

Hydrothermal Plume Detection

Distinct buoyant plume signals were detected rising from the VDVF by anomalous temperature and Eh signals in the water column at depths >2180 mbsl (\sim 180 m above the seafloor) (Figure 2). A secondary plume signal was detected at depths <2180 mbsl with a distinct Eh anomaly and water warmer than background seawater by 0.05°C. We were unable to distinguish non-buoyant plume features typical of Atlantic plumes such as entrainment of cooler deep waters to shallower depths (Rona and Speer, 1989; Speer and Rona, 1989). There was a lack of significant light scattering anomalies throughout the water column, which is unsurprising given the clear appearance of fluids exiting vents. This feature has been noted previously and may be a critical reason for the lack of discovery of similar systems (Connelly et al., 2012; Hodgkinson et al., 2015). The plume seemed to be dispersed in various directions, however, the Niskin rosette was subject to strong currents moving it west-northwest of the ship so this was considered the predominant direction of dispersion at the time of sampling.

Fe and Mn Concentrations in the Plume

Total dissolvable concentrations of Mn (TDMn) and Fe (TDFe) in the VDVF plume were all elevated above NADW concentrations (0.1 nmol kg⁻¹ dMn, 0.75 nmol kg⁻¹ dFe) and measured background dFe (1.1 \pm 0.2 nmol kg⁻¹) suggesting addition of metals to the plume from vent fluids of the VDVF (Table 1, Figure 2 and Supplementary Table S3). The highest dMn and TDMn concentrations were observed in samples >2180 mbsl taken in waters with distinctive temperature, salinity,

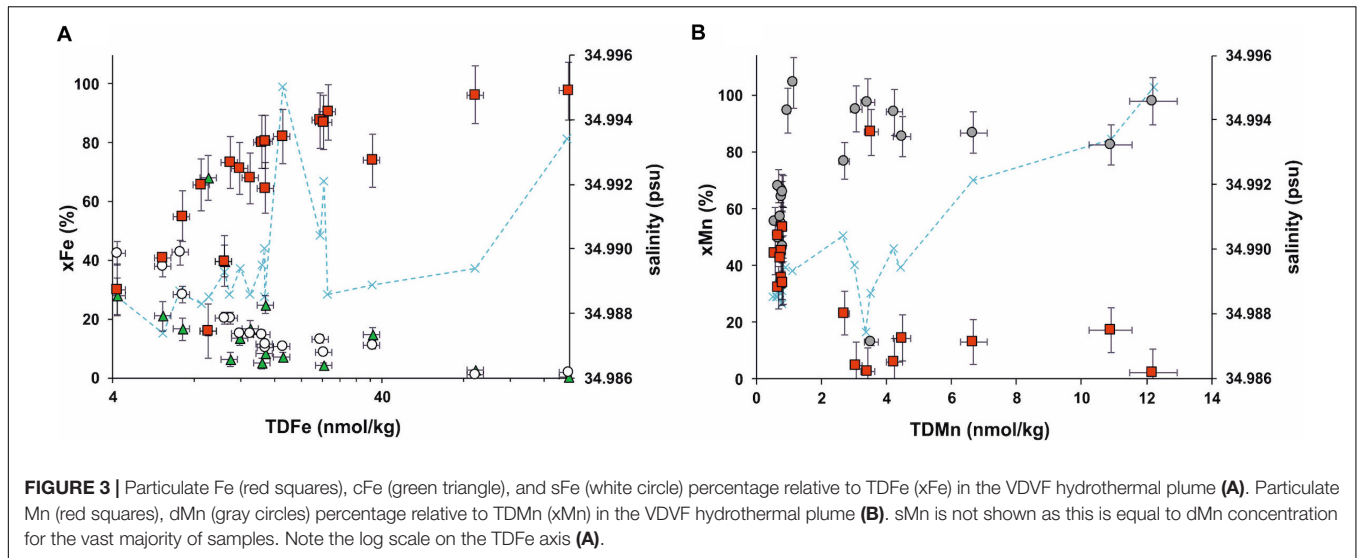
and Eh signals, compared to background seawater but closer to the hydrothermal source at the seafloor (Figure 2). In this study samples with dMn concentrations >0.6 nmol kg⁻¹ had dMn values 92 \pm 8% ($n = 10$) relative to TDMn (Figure 3B). However, samples with dMn concentrations <0.6 nmol kg⁻¹ had only 54 \pm 16% ($n = 10$) dMn relative to TDMn. These samples with a lower percentage of dMn coincided with the lower sample salinity (Figure 3B) and lower temperature region of the plume.

Total dissolvable Fe in the VDVF plume ranged from 4.2 to 196 nmol kg⁻¹ ($n = 20$) with highest concentrations observed in the deeper samples closest to the vents on the seafloor (Figure 2 and Supplementary Table S3). This range of TDFe concentration is similar to that observed from black smoker plumes over a similar distance using the comparable sampling methods as on the East Pacific Rise [TDFe <380 nmol kg⁻¹ (Field and Sherrell, 2000)], the Mid-Atlantic Ridge [TDFe <170 nmol kg⁻¹ from TAG and Broken Spur sites (James and Elderfield, 1996)] and the East Scotia Ridge [TDFe <230 nmol kg⁻¹ (Hawkes et al., 2013)]. Our results are consistent with previous analysis of pFe concentrations (collected on 0.2 μ m filters) at this site in the range of 32 to 320 nmol kg⁻¹ from 2254 to 2296 m (this study = 1.2 to 191 nmol kg⁻¹ pFe). In contrast to what would be expected from plume dispersion, concentrations of dFe and sFe were highest (4.2 and 9.6 nmol kg⁻¹, respectively) in the samples at shallower depths (2091 to 2288 mbsl) (Supplementary Table S3) collected from regions of lower salinity, Eh and temperature compared to background seawater (Figure 2). As a percentage of TDFe (xFe%) the pFe decreases relative to the cFe and sFe fractions (Figure 3A). In contrast to Mn this change appears unrelated to sample salinity (or temperature or Eh) and therefore plume dispersion.

Hydrothermal Plume Particle Composition

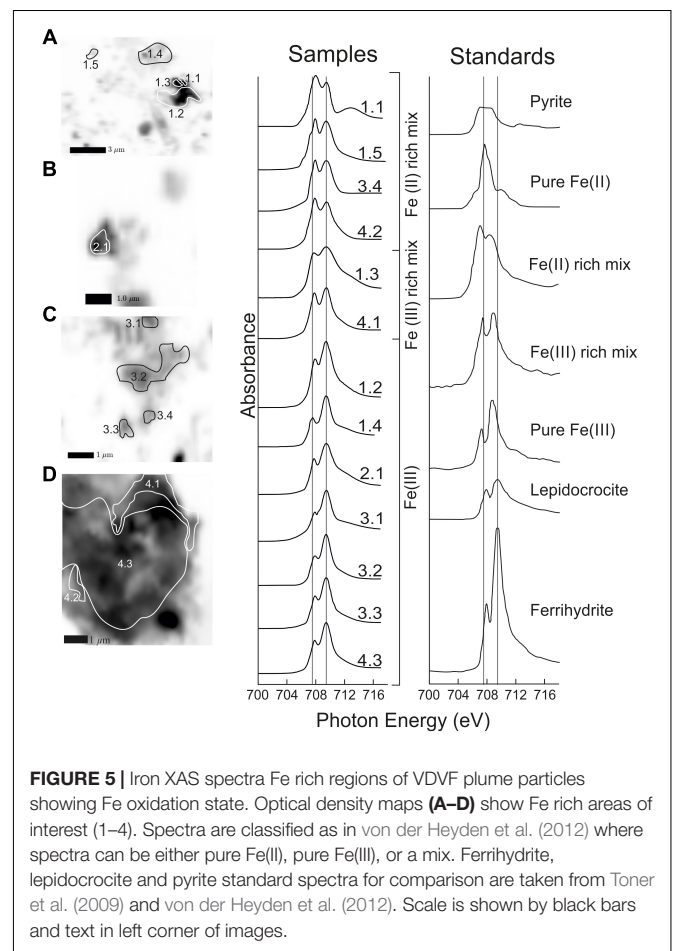
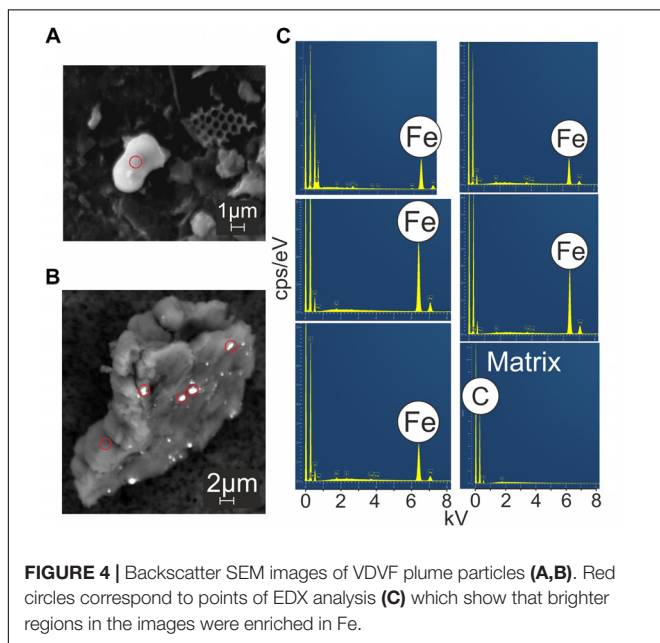
No Fe sulfide particles were discovered during our SEM-EDX analysis session (Supplementary Table S2). Both a solitary rounded Fe rich particle and Fe rich particles embedded in a larger particle made up of low mass elements (i.e., C and O) were observed (Figure 4). The Fe rich particles embedded within the larger particle (\sim 16 μ m) were \sim 1 μ m in size (Figure 4B). The composition of the larger particle matrix (Figure 4B) could not be identified quantitatively as it only showed peaks for lighter elements C, O and trace Si, which give high uncertainties on EDX spectra (Goldstein et al., 2003). The lack of higher mass elements in the larger particle suggests that it maybe organic rather than inorganic.

Several regions with significant absorption peaks at the Fe L_3 edge were identified from X-ray transmission images taken at 710 eV [Fe(III) peak] (Figure 5). The majority of regions examined were classified as pure Fe (III) or Fe(III) rich (Figure 5). Four regions showed an initial Fe(II) peak greater than the Fe(III) peak indicating these regions were enriched in Fe(II) relative to Fe(III). These four regions are small discrete areas located toward the edge of particle aggregates. Whilst the regions enriched in Fe(II) were small as they occurred in three out of four samples examined they are likely a common feature of the plume particles.



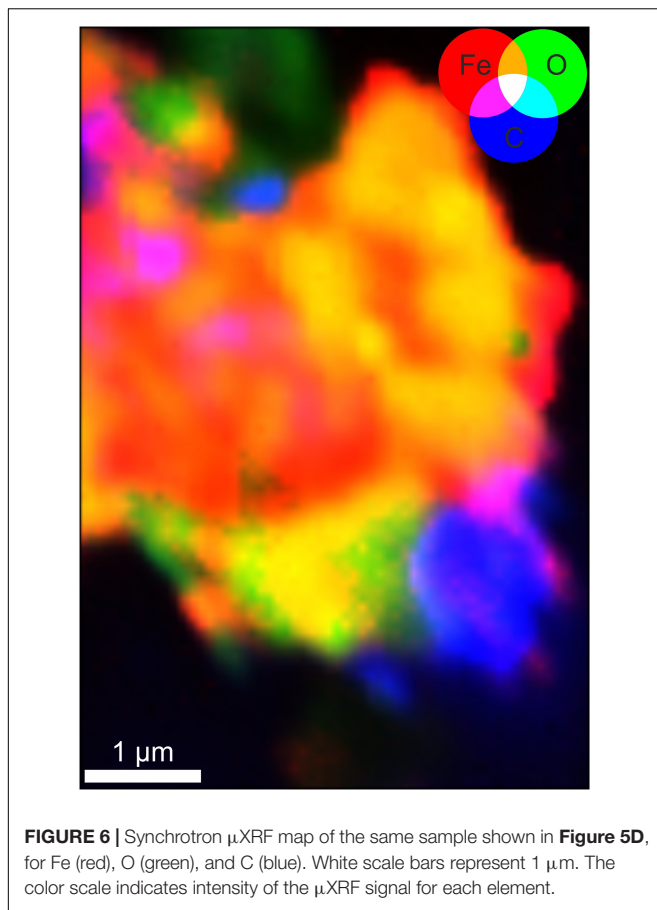
Similar to our SEM-EDX results there were no spectra that were similar to pyrite which does not show a split peak at the Fe L_3 edge as other Fe oxyhydroxide minerals do (Figure 5).

The particle shown in Figure 5D was analyzed using μ XRF to create maps of Fe, O, and C distribution (Figure 6). Oxygen appears to be ubiquitous throughout the particle and the Fe map was similar with the most enriched region to the bottom right. Hence large regions of the particle appear yellow in the image where the red Fe areas overlap with green O areas. In contrast the regions enriched in C appear to the bottom right and upper left of the particle (Figure 6). Within these carbon-enriched regions there are several areas that appear purple-pink in the color map from the co-location of Fe (red) and C (blue). C is located round the margins of the particle similar to regions enriched in Fe (II).



DISCUSSION

Over short distances of several kilometers and time scales of weeks, Mn^{2+} emitted from vent fluids behaves conservatively in



hydrothermal plumes due to its slow oxidation rate (Cowen et al., 1990; Cowen and Li, 1991) and ligand complexation (Madison et al., 2013; Luther et al., 2015; Oldham et al., 2015, 2017). This means that typically in black smoker plumes >80% of Mn in hydrothermal plume samples is found in the dissolved fraction even for samples collected several kilometers away from the vent source (James and Elderfield, 1996; Field and Sherrell, 2000; Lough et al., 2017, 2019). The concentrations of VDVF samples are higher than NADW for both dFe and dMn and Cayman deep water for dFe (lowest plume concentrations are $0.33 \text{ nmol kg}^{-1}$ dMn and 2.4 nmol kg^{-1} dFe compared to 0.1 nmol kg^{-1} dMn and 0.8 nmol kg^{-1} dFe NADW and 1.1 nmol kg^{-1} dFe for Cayman deep waters, respectively). However, the percentage of TDMn present as pMn suggests non-conservative behavior of dMn in the VDVF plume (**Figure 3B**). Given the close proximity of our samples to the vent site it is unlikely that the plume waters have aged more than several weeks since the time of venting. A deep ocean current of 0.1 m s^{-1} (Gordon, 1967) would take 7 h to spread the plume laterally across the section distance (0.5 km) we have sampled, this suggests the sampled plume was hours old rather than days or weeks. This makes it unlikely that the slow rate of Mn oxidation will have oxidized enough of the dMn to form a significant concentration of pMn. What is more likely is that some Mn oxidation has already taken place in the subsurface as a result of seawater-vent fluid mixing prior to venting at the

seafloor. Hence the pMn formed from Mn oxidation can be seen in our lower salinity more dispersed plume samples even though they are taken within 1 km of the vent field (**Figure 3B**). The only other explanation could be enhanced oxidation of Mn by bacteria (Cowen et al., 1990), however, we have no biological information to prove or disprove this and given the high pH of the vent fluids (**Table 1**) the early on-set of Mn^{2+} oxidation prior to venting seems to be the most likely explanation.

Intriguingly the size fractionation of Fe relative to TDFe shows the opposite profile to Mn where sFe and cFe constitute an increasing proportion of TDFe as TDFe decreases (**Figure 3A**). This is counterintuitive as we would expect particle formation within the plume to lower the proportion of sFe and cFe and increase the proportion of pFe. There are three explanations for this increase of cFe and sFe that can be considered. The first is that an additional source of Fe has added sFe and cFe to the VDVF plume without additional pFe. The second explanation is that there is a loss of pFe from particle settling increasing the proportion of cFe and sFe relative to decreasing TDFe. Thirdly the transfer of Fe from pFe to sFe and cFe fractions could explain an increase in sFe and cFe relative to pFe as a result of the breakdown of lithogenic or organic Fe rich particles within the plume.

If the additional sFe and cFe is derived from another Fe source, then given the depth and location of sampling it would have to be from another vent field as the VDVF is too far away from a continental shelf to be influenced by a sedimentary Fe source (**Figure 1**), and too far from the surface to be influenced by atmospheric deposition. This region of the MCSC has been surveyed and there is only one other vent field that has been observed along the MCSC, the Beebe Vent Field (BVF) (German et al., 2010; Connelly et al., 2012) which is located 20 km Northeast of the VDVF. The BVF is the world's deepest active vent site, located at depths of >4950 m with a plume that rises to a depth of 4000 mbsl. This is deeper than the base of the OCC upon which the VDVF sits (**Figure 1B**) and given that the BVF vents sit at the bottom of the axial valley the plume is likely to be constrained by the axial valley walls. Our plume sampling depths ranged from 2300 to 1800 mbsl so it is unlikely that Fe from the BVF plume could have been mixed into the plume over the VDVF. Alternatively, given the range of Fe concentrations measured in Von Damm vent fluids (6.58 to $604 \mu\text{mol kg}^{-1}$; **Table 1**), it could be that changes in the Fe size fractionation of the plume reflect the variability of the VDVF Fe sources. This also seems unlikely given that the majority of plume waters (95% based on flow rate in **Table 1**) will have been sourced from hotter than hole, which also has the highest concentrations of Fe in vent fluids (**Table 1**). It could also be that the increase in the proportion of sFe and cFe is simply the result of mixing plume waters with background seawater that has less pFe. Using background seawater values (**Supplementary Table S1**) the sample with the lowest dFe concentration of 2.4 nmol kg^{-1} is still only 48% background seawater dFe so this is unlikely to explain the entirety of the increase in cFe and sFe. We therefore suggest it is unlikely that Fe additions to the plume from other vent fields, separate vents on the VDVF or background seawater can

explain the increasing proportions of sFe and cFe relative to TDFe (**Figure 3A**).

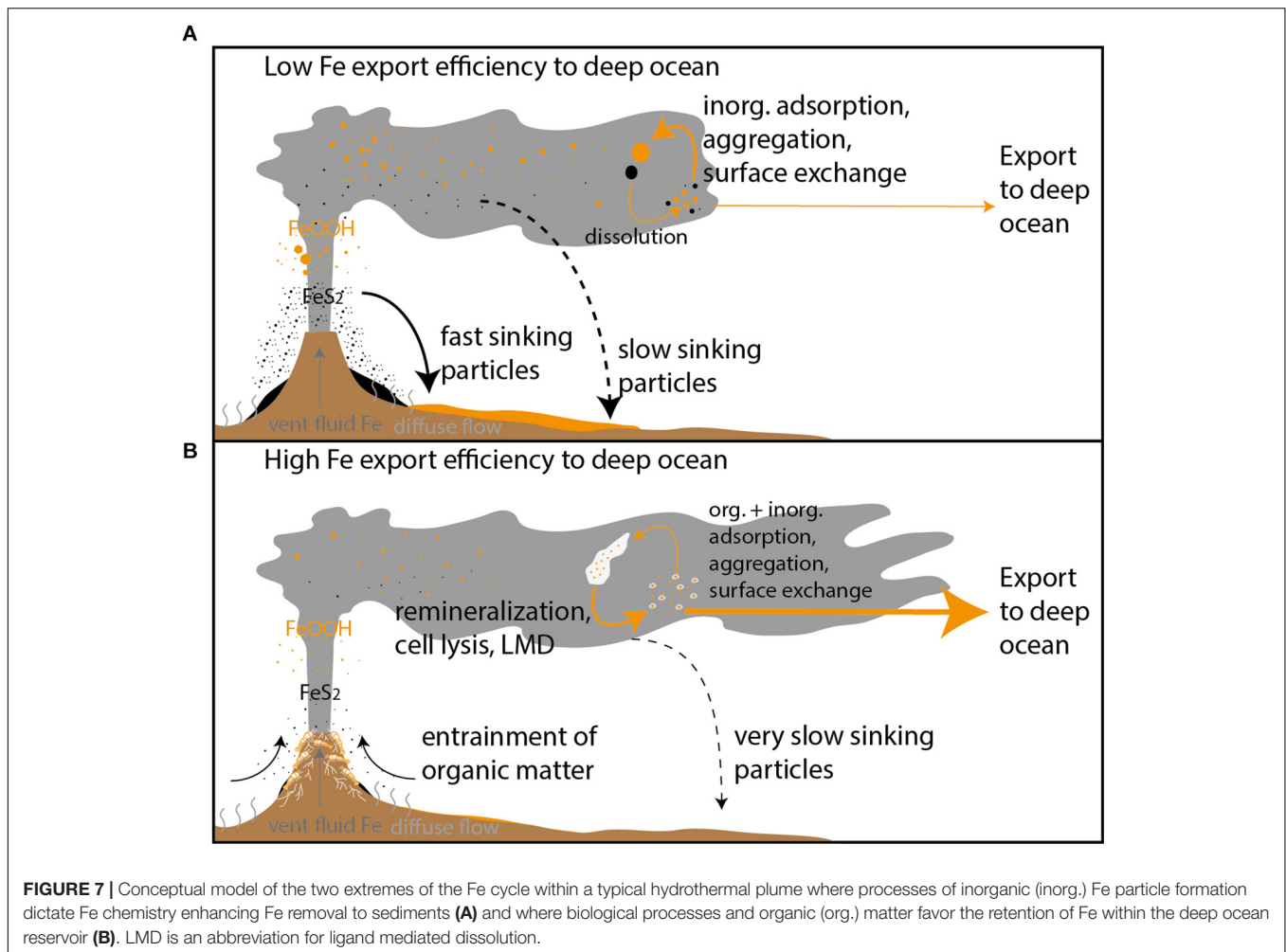
The second alternative explanation for increasing proportions of sFe and cFe is a loss of pFe relative to sFe and cFe as a result of particle settling. We did not observe any Fe sulfides in plume particles examined by microscopy (**Figures 4, 5** and **Supplementary Table S2**) that would settle rapidly according to Stokes' law, due to the density of Fe sulfide minerals $>0.2 \mu\text{m}$. This is further supported by the lack of any visible "black smoke" coming from the vents (Connelly et al., 2012; Hodgkinson et al., 2015), which is usually caused by Fe sulfide particles. We therefore suggest that rapidly settling Fe-sulfide particles make up a minor amount of plume pFe and therefore a negligible amount of venting Fe is removed to sediments by settling of these particles. The particles observed by our microscopy techniques are most likely to be Fe oxyhydroxides given the XANES spectra are similar to that of ferrihydrite and lepidocrocite (**Figure 5**), EDX spectra only showed significant peaks for Fe (**Figure 4**) and μXRF maps show a significant overlap in Fe and O (**Figure 6**). Furthermore, the calculated Fe (II) oxidation half-life at this site is 0.45 h (**Supplementary Table S1**) which will result in rapid conversion of Fe^{2+} to Fe^{3+} and precipitation as Fe-oxyhydroxides similar to that of plumes in the N. Atlantic Ocean (Field and Sherrell, 2000; Santana-González et al., 2017). The largest of the Fe particles examined were approximately spherical and $\sim 5 \mu\text{m}$ in diameter (**Figures 4B, 5D**) which based on Stokes' law would equate to a settling rate of 2.05 m d^{-1} . This can be considered a maximum possible settling rate given many of the Fe particles were $<5 \mu\text{m}$ in diameter and in some cases associated with less dense C matrices. Given the slow settling time of FeOOH particles relative to the hours old plume, we deem it unlikely that a significant amount of pFe has been lost from the plume by settling within a 0.5 km distance of the vent site. Furthermore, pore water dFe concentrations of the Von Damm sediments are in the range of $0\text{--}2 \mu\text{mol kg}^{-1}$ (**Supplementary Figure S1** and **Supplementary Table S4**) which is similar to open ocean Western Atlantic sediments [$0\text{--}7 \mu\text{mol kg}^{-1}$ (Bridgestock et al., 2018)], and less than that found in volcanic sediment [$0\text{--}82 \mu\text{mol kg}^{-1}$ (Homoky et al., 2011)], sediment overlying active submarine volcanism [$0\text{--}575 \mu\text{mol kg}^{-1}$ (Aquilina et al., 2014)] or metal rich sediments surrounding black smoker vents [$0\text{--}3716 \mu\text{mol kg}^{-1}$ (**Supplementary Figure S1** and **Supplementary Table S4**)]. This leads us to believe that there is a negligible loss of Fe from the plume as a result of settling particles within our range of sampling.

After removing the previous two explanations for increasing proportions of sFe and cFe in the VDVF plume we are left with the possibility of transfer of Fe from the particulate fraction to the soluble and colloidal fractions. This would require the breakdown of either Fe bearing POC (Toner et al., 2009; Hoffman et al., 2018) matrices or dissolution of authigenic hydrothermal Fe minerals (Feely et al., 1987; **Figure 7**). The data on the particles we have collected suggests that most of the pFe in the plume is in the form of Fe oxyhydroxides. It is also possible that there is Fe adsorbed to the surface of POC (Toner et al., 2009; Hoffman et al., 2018) and/or mineral particles that was

present but undetected by our methods. Fe oxyhydroxides will be stable in oxygenated seawater and unlikely to undergo dissolution unless this process is ligand mediated. The concentration of Fe binding ligands in the N. Atlantic is $\sim 2.5 \text{ nM}$ (Buck et al., 2015), assuming the concentration is similar in the Caribbean Sea, a portion of our dFe must be present as colloidal Fe oxyhydroxides and/or Fe sulfides as all the measured plume dFe is $>2.5 \text{ nM}$.

Microbial activity in the VDVF plume has the potential to produce ligand-complexed Fe, either by the release of siderophores or by the breakdown of dead microbes and release of intracellular Fe (Muller et al., 2005; Homann et al., 2009; Li et al., 2014; Kleint et al., 2016). Previous work has measured concentrations of elevated POC (130 to 570 nmol kg^{-1} near the vent source, compared to background values of 44 to 90 nmol kg^{-1}) in the VDVF plume (Breier et al., 2014) as a result of entraining organic matter from the communities surrounding the vents. It's possible that the higher pH of the VDVF fluids makes the immediate plume a more hospitable environment to marine microbes in comparison to black smoker vents with lower pH. If the particle investigated by SEM-EDX (**Figure 4B**) is assumed to be organic and representative of particles in the VDVF plume, then the remineralization of these larger Fe bearing particles could increase the concentrations of cFe and sFe in the plume and would lower pFe concentrations. This is consistent with the decreasing pFe and increasing cFe and sFe as a percentage of TDFe (**Figure 3A**).

The fraction of dFe present as cFe in the VDVF plume ($46 \pm 19\%$ cFe) is similar to that observed for a plume in the Scotia Sea from the E9 vent field ($47 \pm 25\%$ cFe) and the nearby BVF plume (35 ± 13) (Lough et al., 2019). Colloidal Fe was higher than that observed by Nishioka et al. (2013) in a plume in the Indian Ocean (23% cFe) where the majority of hydrothermal dFe is in the soluble fraction but lower than the $82\text{--}96\%$ observed over the MAR (Fitzsimmons et al., 2015) and the $71 \pm 15\%$ observed in an island arc caldera rich in aged hydrothermal plume material (Hawkes et al., 2014). The difference in the separation of dFe between cFe and sFe at different sites is further indication that processes generating cFe vary between hydrothermal plumes. Whilst being a unique site the style of venting from the VDVF is analogous to that from diffuse venting around black smokers. It is possible that some of the variation between the size fractionation of Fe in plumes and the fraction of chemically stabilized hydrothermal Fe may not only be a result of differences in inorganic chemistry but differences in organic chemistry. Where the extent to which diffuse fluids rich in organic matter are entrained into the plume facilitates Fe ligand complexation and ultimately how much hydrothermal Fe remains in the deep ocean (**Figure 7**; Sander and Koschinsky, 2011). This hypothesis is consistent with a recent attempt to model the relationship between Fe and organic C which indicates shows that the majority of Fe supplied to hydrothermal plumes comes from the entrainment of diffuse flow (German et al., 2015). We therefore suggest that all hydrothermal plumes lie on a scale between two extremes, which are illustrated in **Figure 7**. In **Figure 7B** the export efficiency of Fe from the



plume to the deep ocean is enhanced by the entrainment and degradation of organic matter from diffuse areas. Without the entrainment and degradation of organic matter the Fe plume chemistry is dominated by inorganic colloids which aggregate to larger denser particles decreasing Fe export to the deep ocean (**Figure 7A**).

Due to the low light scattering profile of the VDVF plume and the widespread occurrence of ocean core complexes it has been suggested that venting similar to that occurring at the VDVF could be active at other slow to ultra-slow spreading ridges (D’Orazio et al., 2004; Hodgkinson et al., 2015). These types of vent fields may remain undetected due to a combination of low level plume particle anomalies, unexplored areas of the deep sea and the bias toward searching ridge axis for plume signals rather than off-axis areas (German et al., 2011). In order to get a true global estimate of how important off-axis venting maybe for Fe fluxes, more information is required on the global occurrence of off-axis vent sites. Importantly, these off-axis sites would not be included in models of hydrothermal dFe input based on ridge spreading rate (Tagliabue et al., 2010). This therefore supports the idea that initial models of hydrothermal dFe input are likely to be a conservative minimum estimate (Saito et al., 2013).

CONCLUSION

Despite the Fe concentration in the hydrothermal vent fluids being at the lower end of the global range (**Table 1**), the VDVF plume has a similar range of TDFe concentrations (VDVF = 4 to 196 nmol kg⁻¹) comparable to plumes directly over ridge axes sampled within a similar distance from the vent source (James and Elderfield, 1996; Hawkes et al., 2013, 2014). This result is counterintuitive to the appearance of the plumes exiting the vents as it was expected that the plume would contain far less pFe due to the lack of significant particle anomalies in the water column.

Given the VDVF plume has a similar range of TDFe concentrations compared to black smoker plumes but the relative amounts of sFe and cFe increase as pFe decreases it is clear from the plume profile that the processes of Fe(II) oxidation, Fe oxyhydroxide formation and colloid formation/aggregation are not expressed in the same way. The VDVF plume gains sFe and cFe relative to TDFe suggesting more conserved dFe concentrations throughout plume dispersion compared to other vent sites and this indicates that there may be additional stabilization processes (**Figure 7**). It cannot be said definitely what these processes are from the results presented here, but the

influence of Fe oxyhydroxide colloid formation and Fe ligand complexation on the concentrations of Fe in the VDVF plume are discussed. We suggest that the most likely explanation for the gain in cFe and sFe is that biologically mediated processes (such as incorporation of Fe into particulate organic matter with subsequent release of organic complexed cFe and sFe) play a more significant role in the VDVF plume resulting in efficient transfer and stabilization of Fe in the overlying plume facilitating export to the deep ocean (Figure 7). This would be in contrast to black smoker type plumes where inorganic processes of colloid and particle formation are more likely to dictate Fe plume chemistry. The VDVF plume therefore serves as an ideal natural laboratory for exploring how the hydrothermal flux of trace metals is controlled by interactions between trace metals and organic carbon. Future work at this site should aim to make more extensive measurements of POC concentration and dFe ligand binding strength to test the ideas we have presented here further.

The VDVF plume represents a previously unrecognized source of off-axis hydrothermal dFe, which could be present in other ocean basins. The formation sFe and cFe in the VDVF plume could also be analogous to that occurring in diffuse areas of venting around black smoker vents. This diffuse venting is also mixed into the plume and therefore could be an important mechanism for stabilizing dFe globally as has been proposed previously in a model of hydrothermal Fe and organic C (German et al., 2015).

DATA AVAILABILITY

The datasets generated for this study are available on request to the corresponding author. Trace metal concentrations data are provided in the supplementary information. All data is available from the lead authors personal webpage https://www.researchgate.net/profile/Alastair_Lough and CTD data is available from the British oceanographic data centre <https://www.bodc.ac.uk/>.

AUTHOR CONTRIBUTIONS

AJML, DPC, WBH, JAH, and RAM contributed to the conception and design of the study. Funding for the JC82 voyage and sample analysis was secured by DPC. Fieldwork was undertaken by AJML, WBH, JAH, VC, AC, and RAM. K-iN provided the

Eh sensor for detecting the hydrothermal plume and advised AJML with regards to data processing and interpretation. AJML performed the trace metal analysis of plume samples and processed ICP-MS, sensor, SEM-EDX and soft X-ray spectromicroscopy data. Spectromicroscopy data was acquired by BK, MK, and TA who advised AJML in data processing and interpretation of both spectromicroscopy and SEM-EDX data. Pore water trace metal data was analyzed and processed by WBH and RAM. AJML wrote the first draft of the manuscript with all authors contributing to manuscript revisions and approving submission of the final version. AJML wrote the manuscript and prepared the figures with co-authors reviewing and providing comments on drafts.

FUNDING

The JC82 voyage was supported by the Natural Environment Research Council funding (NERC United Kingdom Grants NE/F017758/1 and NE/F017774/1). The work of AJML was funded by the NERC, United Kingdom Ph.D. Studentship NE/K500938/1. WBH was additionally supported by an NERC Fellowship NE/K009532/1. Plume particles were analyzed at the Diamond Light Source (United Kingdom) using the I08 beam line, experiment number SP12738. VC and AC acknowledge the financial CNRS – INSU grants “Post-campagne: JC82 Cayman Ridge” and “TelluS-SYSTER: LIMOR.”

ACKNOWLEDGMENTS

We thank the master and crew of the *RRS James Cook* and the pilots and technical team of the ROV *Isis*. We also thank M. Cooper for his help in analyzing the vent fluids and pore waters and JA Milton for his help in ICP-MS analysis. We would also like to thank Richard Pearce for his help in SEM-EDX analysis. We would like to thank the editor and both the reviewers for their helpful comments in improving this manuscript for publication.

SUPPLEMENTARY MATERIAL

The Supplementary Material for this article can be found online at: <https://www.frontiersin.org/articles/10.3389/fmars.2019.00329/full#supplementary-material>

REFERENCES

- Aquilina, A., Homoky, W. B., Hawkes, J. A., Lyons, T. W., and Mills, R. A. (2014). Hydrothermal sediments are a source of water column Fe and Mn in the bransfield strait Antarctica. *Geochim. Cosmochim. Acta* 137, 64–80. doi: 10.1016/j.gca.2014.04.003
- Baker, E. T., Resing, J. A., Haymon, R. M., Tunnicliffe, V., Lavelle, J. W., Martinez, F., et al. (2016). How many vent fields? New estimates of vent field populations on ocean ridges from precise mapping of hydrothermal discharge locations. *Earth Planet. Sci. Lett.* 449, 186–196. doi: 10.1016/j.epsl.2016.05.031
- Bennett, S. A., Achterberg, E. P., Connelly, D. P., Statham, P. J., Fones, G. R., and German, C. R. (2008). The distribution and stabilisation of dissolved Fe in deep-sea hydrothermal plumes. *Earth Planet. Sci. Lett.* 270, 157–167. doi: 10.1016/j.epsl.2008.01.048
- Billier, D. V., and Bruland, K. W. (2012). Analysis of Mn, Fe, Co, Ni, Cu, Zn, Cd, and Pb in seawater using the Nobias-chelate PA1 resin and magnetic sector inductively coupled plasma mass spectrometry (ICP-MS). *Mar. Chem.* 130, 12–20. doi: 10.1016/j.marchem.2011.12.001
- Breier, J. A., Sheik, C. S., Gomez-Ibanez, D., Sayre-McCord, R. T., Sanger, R., Rauch, C., et al. (2014). A large volume particulate and water multi-sampler with in situ preservation for microbial and biogeochemical studies. *Deep Sea Res. Part I Oceanogr. Res. Pap.* 94, 195–206. doi: 10.1016/j.dsr.2014.08.008
- Bridgestock, L., Hsieh, Y.-T., Porcelli, D., Homoky, W. B., Bryan, A., and Henderson, G. M. (2018). Controls on the barium isotope compositions of

- marine sediments. *Earth Planet. Sci. Lett.* 481, 101–110. doi: 10.1016/j.epsl.2017.10.019
- Buck, K. N., Sohst, B., and Sedwick, P. N. (2015). The organic complexation of dissolved iron along the US GEOTRACES (GA03) North Atlantic Section. *Deep Sea Res. Part II Top. Stud. Oceanogr.* 116, 152–165. doi: 10.1016/j.dsr2.2014.11.016
- Butterfield, D. A., Nakamura, K., Takano, B., Lilley, M. D., Lupton, J. E., Resing, J. A., et al. (2011). High SO₂ flux, sulfur accumulation, and gas fractionation at an erupting submarine volcano. *Geology* 39, 803–806. doi: 10.1130/g31901.1
- Connelly, D. P., Copley, J. T., Murton, B. J., Stansfield, K., Tyler, P. A., German, C. R., et al. (2012). Hydrothermal vent fields and chemosynthetic biota on the world's deepest seafloor spreading centre. *Nat. Commun.* 3:620. doi: 10.1038/ncomms1636
- Conway, T. M., and John, S. G. (2014). Quantification of dissolved iron sources to the North Atlantic Ocean. *Nature* 511, 212–215. doi: 10.1038/nature13482
- Copley, J. T., and Talling, J. T. (2013). *RRS James Cook JC082cruise Inventory*. JC083 Cruise Report. Liverpool: British Oceanographic Data Centre.
- Cowen, J. P., and Li, Y. H. (1991). The influence of changing bacterial community on trace metal scavenging in a deep sea particle plume. *J. Mar. Res.* 49, 517–542. doi: 10.1357/002224091784995800
- Cowen, J. P., Massoth, G. J., and Feely, R. A. (1990). Scavenging rates of dissolved manganese in a hydrothermal plume. *Deep Sea Res. Part A Oceanogr. Res. Pap.* 37, 1619–1637. doi: 10.1016/0198-0149(90)90065-4
- de Groot, F. M. F. (2009). XANES spectra of transition metal compounds. *J. Phys. Conf. Ser.* 190:9.
- D'Orazio, M., Boschi, C., and Brunelli, D. (2004). Talc-rich hydrothermal rocks from the St. Paul and Conrad fracture zones in the Atlantic Ocean. *Eur. J. Mineral.* 16, 73–83. doi: 10.1127/0935-1221/2004/0016-0073
- Elderfield, H., and Schultz, A. (1996). Mid-ocean ridge hydrothermal fluxes and the chemical composition of the ocean. *Annu. Rev. Earth Planet. Sci.* 24, 191–224. doi: 10.1146/annurev.earth.24.1.191
- Escartin, J., Mével, C., Petersen, S., Bonnemains, D., Cannat, M., Andreani, M., et al. (2017). Tectonic structure, evolution, and the nature of oceanic core complexes and their detachment fault zones (13°20'N and 13°30'N, Mid Atlantic Ridge). *Geochem. Geophys. Geosyst.* 18, 1451–1482. doi: 10.1002/2016gc006775
- Escartin, J., Smith, D. K., Cann, J., Schouten, H., Langmuir, C. H., and Escrig, S. (2008). Central role of detachment faults in accretion of slow-spreading oceanic lithosphere. *Nature* 455:790. doi: 10.1038/nature07333
- Feely, R. A., Gendron, J. F., Baker, E. T., and Lebon, G. T. (1994). Hydrothermal plumes along the east pacific rise, 8-degrees-40' to 11-degrees-50'N - particle distribution and composition. *Earth Planet. Sci. Lett.* 128, 19–36. doi: 10.1016/0012-821x(94)90023-x
- Feely, R. A., Lewison, M., Massoth, G. J., Robertbaldo, G., Lavelle, J. W., Byrne, R. H., et al. (1987). Composition and dissolution of black smoker particulates from active vents on the Jaun de fuca ridge. *J. Geophys. Res. Solid Earth Planets* 92, 11347–11363. doi: 10.1029/jb092ib11p11347
- Field, M. P., and Sherrell, R. M. (2000). Dissolved and particulate Fe in a hydrothermal plume at 9 degrees 45' N, east pacific rise: slow Fe (II) oxidation kinetics in Pacific plumes. *Geochim. Cosmochim. Acta* 64, 619–628. doi: 10.1016/s0016-7037(99)00333-6
- Fitzsimmons, J. N., Boyle, E. A., and Jenkins, W. J. (2014). Distal transport of dissolved hydrothermal iron in the deep south pacific ocean. *Proc. Natl. Acad. Sci. U.S.A.* 111, 16654–16661. doi: 10.1073/pnas.1418778111
- Fitzsimmons, J. N., Carrasco, G. G., Wu, J. F., Roshan, S., Hatta, M., Measures, C. I., et al. (2015). Partitioning of dissolved iron and iron isotopes into soluble and colloidal phases along the GA03 GEOTRACES North Atlantic transect. *Deep Sea Res. Part II Top. Stud. Oceanogr.* 116, 130–151. doi: 10.1016/j.dsr2.2014.11.014
- Fitzsimmons, J. N., John, S. G., Marsay, C. M., Hoffman, C. L., Nicholas Sarah, L., Toner, B. M., et al. (2017). Iron persistence in a distal hydrothermal plume supported by dissolved–particulate exchange. *Nat. Geosci.* 10:195. doi: 10.1038/ngeo2900
- Gartman, A., Findlay, A. J., and Luther, G. W. (2014). Nanoparticulate pyrite and other nanoparticles are a widespread component of hydrothermal vent black smoker emissions. *Chem. Geol.* 366, 32–41. doi: 10.1016/j.chemgeo.2013.12.013
- German, C. (2016). GEOTRACES royal society meeting on ocean boundary fluxes.
- German, C. R., Bowen, A., Coleman, M. L., Honig, D. L., Huber, J. A., Jakuba, M. V., et al. (2010). Diverse styles of submarine venting on the ultraslow spreading mid-cayman rise. *Proc. Natl. Acad. Sci. U.S.A.* 107, 14020–14025. doi: 10.1073/pnas.1009205107
- German, C. R., Legendre, L. L., Sander, S. G., Niqul, N., Luther, G. W., Bharati, L., et al. (2015). Hydrothermal Fe cycling and deep ocean organic carbon scavenging: model-based evidence for significant POC supply to seafloor sediments. *Earth Planet. Sci. Lett.* 419, 143–153. doi: 10.1016/j.epsl.2015.03.012
- German, C. R., Petersen, S., and Hannington, M. D. (2016). Hydrothermal exploration of mid-ocean ridges: Where might the largest sulfide deposits be forming? *Chem. Geol.* 420, 114–126. doi: 10.1016/j.chemgeo.2015.11.006
- German, C. R., Ramirez-Llodra, E., Baker, M. C., Tyler, P. A., and ChEss Sci Steering Committee (2011). Deep-water chemosynthetic ecosystem research during the census of marine life decade and beyond: a proposed deep-ocean road map. *PLoS One* 6:e23259. doi: 10.1371/journal.pone.0023259
- Goldstein, J., Newbury, D. E., Joy, D. C., Lyman, C. E., Echlin, P., Lifshin, E., et al. (2003). *Scanning Electron Microscopy and X-Ray Microanalysis*. New York, NY: Springer.
- Gordon, A. L. (1967). Circulation of the caribbean Sea. *J. Geophys. Res.* 72, 6207–6223. doi: 10.1029/jz072i024p06207
- Guieu, C., Bonnet, S., Petrenko, A., Menkes, C., Chavagnac, V., Desboeufs, K., et al. (2018). Iron from a submarine source impacts the productive layer of the western tropical south pacific (WTSP). *Sci. Rep.* 8:9075. doi: 10.1038/s41598-018-27407-z
- Hawkes, J. A., Connelly, D. P., Gledhill, M., and Achterberg, E. P. (2013). The stabilisation and transportation of dissolved iron from high temperature hydrothermal vent systems. *Earth Planet. Sci. Lett.* 375, 280–290. doi: 10.1016/j.epsl.2013.05.047
- Hawkes, J. A., Connelly, D. P., Rijkenberg, M. J. A., and Achterberg, E. P. (2014). The importance of shallow hydrothermal island arc systems in ocean biogeochemistry. *Geophys. Res. Lett.* 41, 942–947. doi: 10.1002/2013gl058817
- Hawkes, J. A., Rossel, P. E., Stubbins, A., Butterfield, D., Connelly, D. P., Achterberg, E. P., et al. (2015). Efficient removal of recalcitrant deep-ocean dissolved organic matter during hydrothermal circulation. *Nat. Geosci.* 8:856. doi: 10.1038/ngeo2543
- Hawkings, J. R., Benning, L. G., Raiswell, R., Kaulich, B., Araki, T., Abyaneh, M., et al. (2018). Biolabile ferrous iron bearing nanoparticles in glacial sediments. *Earth Planet. Sci. Lett.* 493, 92–101. doi: 10.1016/j.epsl.2018.04.022
- Hodgkinson, M. R. S., Webber, A. P., Roberts, S., Mills, R. A., Connelly, D. P., and Murton, B. J. (2015). Talc-dominated seafloor deposits reveal a new class of hydrothermal system. *Nat. Commun.* 6:10150. doi: 10.1038/ncomms10150
- Hoffman, C. L., Nicholas, S. L., Ohnemus, D. C., Fitzsimmons, J. N., Sherrell, R. M., German, C. R., et al. (2018). Near-field iron and carbon chemistry of non-buoyant hydrothermal plume particles, southern east pacific rise 15°S. *Mar. Chem.* 201, 183–197. doi: 10.1016/j.marchem.2018.01.011
- Homann, V. V., Sandy, M., Tincu, J. A., Templeton, A. S., Tebo, B. M., and Butler, A. (2009). Loihichelins A-F, a suite of amphiphilic siderophores produced by the marine bacterium halomonas LOB-5. *J. Nat. Prod.* 72, 884–888. doi: 10.1021/np800640h
- Homoky, W. B., Hembury, D. J., Hepburn, L. E., Mills, R. A., Statham, P. J., Fones, G. R., et al. (2011). Iron and manganese diagenesis in deep sea volcanogenic sediments and the origins of pore water colloids. *Geochim. Cosmochim. Acta* 75, 5032–5048. doi: 10.1016/j.gca.2011.06.019
- James, R. H., and Elderfield, H. (1996). Dissolved and particulate trace metals in hydrothermal plumes at the Mid-Atlantic Ridge. *Geophys. Res. Lett.* 23, 3499–3502. doi: 10.1029/96gl01588
- Johns, W. E., Townsend, T. L., Fratantoni, D. M., and Wilson, W. D. (2002). On the Atlantic inflow to the Caribbean Sea. *Deep Sea Res. Part I Oceanogr. Res. Pap.* 49, 211–243. doi: 10.1016/S0967-0637(01)00041-3
- Kelley, D. S., Karson, J. A., Früh-Green, G. L., Yoerger, D. R., Shank, T. M., Butterfield, D. A., et al. (2005). A serpentinite-hosted ecosystem: the lost city hydrothermal field. *Science* 307, 1428–1434. doi: 10.1126/science.1102556
- Kleint, C., Hawkes, J. A., Sander, S. G., and Koschinsky, A. (2016). Voltammetric investigation of hydrothermal iron speciation. *Front. Mar. Sci.* 3:75. doi: 10.3389/fmars.2016.00075
- Lemaitre, N., Bayon, G., Ondréas, H., Caprais, J.-C., Freslon, N., Bollinger, C., et al. (2014). Trace element behaviour at cold seeps and the potential export of dissolved iron to the ocean. *Earth Planet. Sci. Lett.* 404, 376–388. doi: 10.1016/j.epsl.2014.08.014
- Lerotic, M., Mak, R., Wirick, S., Meirer, F., and Jacobsen, C. (2014). MANTiS: a program for the analysis of X-ray spectromicroscopy data. *J. Synchrotron. Radiat.* 21, 1206–1212. doi: 10.1107/S1600577514013964

- Leroy, S., Mauffret, A., Patriat, P., and de Lépinay, B. M. (2000). An alternative interpretation of the Cayman trough evolution from a reidentification of magnetic anomalies. *Geophys. J. Int.* 141, 539–557. doi: 10.1046/j.1365-246x.2000.00059.x
- Li, M., Toner, B. M., Baker, B. J., Breier, J. A., Sheik, C. S., and Dick, G. J. (2014). Microbial iron uptake as a mechanism for dispersing iron from deep-sea hydrothermal vents. *Nat. Commun.* 5:8. doi: 10.1038/ncomms4192
- Lough, A. J. M., Homoky, W. B., Connelly, D. P., Comer-Warner, S. A., Nakamura, K., Abyaneh, M. K., et al. (2019). Soluble iron conservation and colloidal iron dynamics in a hydrothermal plume. *Chem. Geol.* 511, 225–237. doi: 10.1016/j.chemgeo.2019.01.001
- Lough, A. J. M., Klar, J. K., Homoky, W. B., Comer-Warner, S. A., Milton, J. A., Connelly, D. P., et al. (2017). Opposing authigenic controls on the isotopic signature of dissolved iron in hydrothermal plumes. *Geochim. Cosmochim. Acta* 202, 1–20. doi: 10.1016/j.gca.2016.12.022
- Luther, G. W., Madison, A. S., Mucci, A., Sundby, B., and Oldham, V. E. (2015). A kinetic approach to assess the strengths of ligands bound to soluble Mn(III). *Mar. Chem.* 173, 93–99. doi: 10.1016/j.marchem.2014.09.006
- Madison, A. S., Tebo, B. M., Mucci, A., Sundby, B., and Luther, G. W. (2013). Abundant porewater Mn(III) is a major component of the sedimentary redox system. *Science* 341, 875–878. doi: 10.1126/science.1241396
- McCarthy, K. T., Pichler, T., and Price, R. E. (2005). Geochemistry of champagne hot springs shallow hydrothermal vent field and associated sediments dominica, lesser antilles. *Chem. Geol.* 224, 55–68. doi: 10.1016/j.chemgeo.2005.07.014
- Millero, F. J., Sotolongo, S., and Izaguirre, M. (1987). The oxidation kinetics of Fe(II) in seawater. *Geochim. Cosmochim. Acta* 51, 793–801. doi: 10.1016/0016-7037(87)90093-7
- Milne, A., Landing, W., Bizimis, M., and Morton, P. (2010). Determination of Mn, Fe, Co, Ni, Cu, Zn, Cd and Pb in seawater using high resolution magnetic sector inductively coupled mass spectrometry (HR-ICP-MS). *Anal. Chim. Acta* 665, 200–207. doi: 10.1016/j.aca.2010.03.027
- Mottl, M. J., and McConachy, T. F. (1990). Chemical processes in buoyant hydrothermal plumes on the east pacific rise near 21°N. *Geochim. Cosmochim. Acta* 54, 1911–1927. doi: 10.1016/0016-7037(90)90261-i
- Muller, F. L. L., Larsen, A., Stedmon, C. A., and Sondergaard, M. (2005). Interactions between algal-bacterial populations and trace metals in fjord surface waters during a nutrient-stimulated summer bloom. *Limnol. Oceanogr.* 50, 1855–1871. doi: 10.4319/lo.2005.50.6.1855
- Nishioka, J., Obata, H., and Tsumune, D. (2013). Evidence of an extensive spread of hydrothermal dissolved iron in the Indian Ocean. *Earth Planet. Sci. Lett.* 361, 26–33. doi: 10.1016/j.epsl.2012.11.040
- Obata, H., Karatani, H., and Nakayama, E. (1993). Automated determination of iron in seawater by chelating resin concentration and chemiluminescence detection. *Anal. Chem.* 65, 1524–1528. doi: 10.1021/ac00059a007
- Oldham, V. E., Mucci, A., Tebo, B. M., and Luther, G. W. (2017). Soluble Mn(III)–L complexes are abundant in oxygenated waters and stabilized by humic ligands. *Geochim. Cosmochim. Acta* 199, 238–246. doi: 10.1016/j.gca.2016.11.043
- Oldham, V. E., Owings, S. M., Jones, M. R., Tebo, B. M., and Luther, G. W. (2015). Evidence for the presence of strong Mn(III)-binding ligands in the water column of the chesapeake bay. *Mar. Chem.* 171, 58–66. doi: 10.1016/j.marchem.2015.02.008
- Resing, J. A., Sedwick, P. N., German, C. R., Jenkins, W. J., Moffett, J. W., Sohst, B. M., et al. (2015). Basin-scale transport of hydrothermal dissolved metals across the south pacific ocean. *Nature* 523, 200–203. doi: 10.1038/nature14577
- Rijkenberg, M. J. A., Middag, R., Laan, P., Gerringa, L. J. A., van Aken, H. M., Schoemann, V., et al. (2014). The distribution of dissolved iron in the west atlantic ocean. *PLoS One* 9:14. doi: 10.1371/journal.pone.0101323
- Rizzo, A. L., Caracausi, A., Chavagnac, V., Nomikou, P., Polymenakou, P. N., Mandalakis, M., et al. (2016). Kolumbo submarine volcano (Greece): an active window into the aegean subduction system. *Sci. Rep.* 6:28013. doi: 10.1038/srep28013
- Rona, P. A., and Speer, K. G. (1989). An atlantic hydrothermal plume: trans-atlantic geotraverse (TAG) area, mid-atlantic ridge crest near 26°N. *J. Geophys. Res. Solid Earth* 94, 13879–13893. doi: 10.1029/jb094i10p13879
- Saito, M. A., Noble, A. E., Tagliabue, A., Goepfert, T. J., Lamborg, C. H., and Jenkins, W. J. (2013). Slow-spreading submarine ridges in the South Atlantic as a significant oceanic iron source. *Nat. Geosci.* 6, 775–779. doi: 10.1038/ngeo1893
- Sander, S. G., and Koschinsky, A. (2011). Metal flux from hydrothermal vents increased by organic complexation. *Nat. Geosci.* 4, 145–150. doi: 10.1038/ngeo1088
- Santana-Casiano, J. M., Gonzaaez-Davila, M., and Millero, F. J. (2005). Oxidation of nanomolar levels of Fe(II) with oxygen in natural waters. *Environ. Sci. Technol.* 39, 2073–2079. doi: 10.1021/es049748y
- Santana-González, C., Santana-Casiano, J. M., González-Dávila, M., and Fraile-Nuez, E. (2017). Emissions of Fe(II) and its kinetic of oxidation at tagoro submarine volcano, El hierro. *Mar. Chem.* 195, 129–137. doi: 10.1016/j.marchem.2017.02.001
- Schlitzer, R. (2017). *Ocean Data View*. Available at: <https://odv.awi.de/> (accessed December 12, 2018).
- Schlitzer, R. (2002). Interactive analysis and visualization of geoscience data with ocean data view. *Comput. Geosci.* 28, 1211–1218. doi: 10.1016/s0098-3004(02)00040-7
- Severmann, S., Johnson, C. M., Beard, B. L., German, C. R., Edmonds, H. N., Chiba, H., et al. (2004). The effect of plume processes on the Fe isotope composition of hydrothermally derived Fe in the deep ocean as inferred from the rainbow vent site, mid-atlantic ridge, 36°14'N. *Earth Planet. Sci. Lett.* 225, 63–76. doi: 10.1016/j.epsl.2004.06.001
- Smith, D. K., Cann, J. R., and Escartin, J. (2006). Widespread active detachment faulting and core complex formation near 13 degrees N on the mid-atlantic ridge. *Nature* 442, 440–443. doi: 10.1038/nature04950
- Solé, V. A., Papillon, E., Cotte, M., Walter, P., and Susini, J. (2007). A multiplatform code for the analysis of energy-dispersive X-ray fluorescence spectra. *Spectrochim. Acta Part B At. Spectrosc.* 62, 63–68. doi: 10.1016/j.sab.2006.12.002
- Speer, K. G., and Rona, P. A. (1989). A model of an Atlantic and pacific hydrothermal plume. *J. Geophys. Res. Oceans* 94, 6213–6220.
- Statham, P. J., German, C. R., and Connelly, D. P. (2005). Iron(II) distribution and oxidation kinetics in hydrothermal plumes at the kairei and edmond vent sites, indian ocean. *Earth Planet. Sci. Lett.* 236, 588–596. doi: 10.1016/j.epsl.2005.03.008
- Tagliabue, A., Bopp, L., Dutay, J., Bowie, A. R., Chever, F., Jean-Baptiste, P., et al. (2010). Hydrothermal contribution to the oceanic dissolved iron inventory. *Nature* 463, 252–256. doi: 10.1038/ngeo818
- Tagliabue, A., and Resing, J. (2016). Impact of hydrothermalism on the ocean iron cycle. *Philos. Trans. A Math. Phys. Eng. Sci.* 374:20150291. doi: 10.1098/rsta.2015.0291
- Tivey, M. K., Humphris, S. E., Thompson, G., Hannington, M. D., and Rona, P. A. (1995). Deducing patterns of fluid flow and mixing within the TAG active hydrothermal mound using mineralogical and geochemical data. *J. Geophys. Res. Solid Earth* 100, 12527–12555. doi: 10.1029/95jb00610
- Toner, B. M., Fakra, S. C., Manganini, S. J., Santelli, C. M., Marcus, M. A., Moffett, J., et al. (2009). Preservation of iron(II) by carbon-rich matrices in a hydrothermal plume. *Nat. Geosci.* 2, 197–201. doi: 10.1038/ngeo433
- Toner, B. M., German, C. R., Dick, G. J., and Breier, J. A. (2016). Deciphering the complex chemistry of deep-ocean particles using complementary synchrotron X-ray microscope and microprobe instruments. *Acc. Chem. Res.* 49, 128–137. doi: 10.1021/acs.accounts.5b00282
- Toner, B. M., Nicholas, S. L., and Wasik, J. K. C. (2014). Scaling up: fulfilling the promise of X-ray microprobe for biogeochemical research. *Environ. Chem.* 11, 4–9.
- Vic, C., Gula, J., Roulet, G., and Pradillon, F. (2018). Dispersion of deep-sea hydrothermal vent effluents and larvae by submesoscale and tidal currents. *Deep Sea Res. Part I* 133, 1–18. doi: 10.1016/j.dsr.2018.01.001
- Von Damm, K. L. (1990). Seafloor hydrothermal activity - black smoker chemistry and chimneys. *Annu. Rev. Earth Planet. Sci.* 18, 173–204. doi: 10.1146/annurev.earth.18.1.173
- Von Damm, K. L. (1995). Temporal and compositional diversity in seafloor hydrothermal fluids. *Rev. Geophys.* 33, 1297–1305. doi: 10.1029/95rg00283
- Von Damm, K. L., Edmond, J. M., Grant, B., and Measures, C. I. (1985). Chemistry of submarine hydrothermal solutions at 21-degrees-N. East Pacific Rise. *Geochim. Cosmochim. Acta* 49, 2197–2220. doi: 10.1016/0016-7037(85)90222-4

- von der Heyden, B. P., Roychoudhury, A. N., Mtshali, T. N., Tyliczszak, T., and Myneni, S. C. B. (2012). Chemically and geographically distinct solid-phase iron pools in the southern ocean. *Science* 338, 1199–1201. doi: 10.1126/science.1227504
- Vondamm, K. L., and Bischoff, J. L. (1987). Chemistry of hydrothermal solutions from the southern Juan de Fuca ridge. *J. Geophys. Res. Solid Earth Planets* 92, 11334–11346. doi: 10.1029/jb092ib11p11334
- Waeles, M., Cotte, L., Pernet-Coudrier, B., Chavagnac, V., Cathalot, C., Leleu, T., et al. (2017). On the early fate of hydrothermal iron at deep-sea vents: a reassessment after in situ filtration. *Geophys. Res. Lett.* 44, 4233–4240. doi: 10.1002/2017gl073315
- Wang, H., Yang, Q., Ji, F., Lilley, M. D., and Zhou, H. (2012). The geochemical characteristics and Fe(II) oxidation kinetics of hydrothermal plumes at the Southwest Indian Ridge. *Mar. Chem.* 13, 29–35. doi: 10.1016/j.marchem.2012.02.009
- Wu, J. F., Wells, M. L., and Rember, R. (2011). Dissolved iron anomaly in the deep tropical-subtropical Pacific: evidence for long-range transport of hydrothermal iron. *Geochim. Cosmochim. Acta* 75, 460–468. doi: 10.1016/j.gca.2010.10.024

Conflict of Interest Statement: The authors declare that the research was conducted in the absence of any commercial or financial relationships that could be construed as a potential conflict of interest.

Copyright © 2019 Lough, Connelly, Homoky, Hawkes, Chavagnac, Castillo, Kazemian, Nakamura, Araki, Kaulich and Mills. This is an open-access article distributed under the terms of the Creative Commons Attribution License (CC BY). The use, distribution or reproduction in other forums is permitted, provided the original author(s) and the copyright owner(s) are credited and that the original publication in this journal is cited, in accordance with accepted academic practice. No use, distribution or reproduction is permitted which does not comply with these terms.